Indirect airflow distribution measurement method for horticultural crop package design

C. Vigneault[1, 2]*, L.R. de Castro[1, 2], B. Goyette[1], N.R. Markarian[1],
M.T. Charles[1], G. Bourgeois[1], E. Tang Line Foot[1] and L.A.B. Cortez[2]

*[1]Horticultural Research and Development Centre, 430 Gouin Blvd., Saint-Jean-sur Richelieu, Quebec J3B 3E6, Canada; and [2]College of Agricultural Engineering, State University of Campinas (UNICAMP), Cidade Universitária Zeferino Vaz, s/n, Campinas, SP, Brazil, CP6011, 13083-970. *Email: vigneaultc@agr.gc.ca.* *[1]Contribution No. 335/2006.02.01R.*

Vigneault, C., de Castro, L.R., Goyette, B., Markarian, N.R., Charles, M.T., Bourgeois, G., Tang Line Foot, E. and Cortez, L.A.B. 2007. **Indirect airflow distribution measurement method for horticultural crop package design.** Canadian Biosystems Engineering/Le génie des biosystèmes au Canada **49**: 3.13 - 3.22. Information about the air flow distribution inside a porous medium such as a container of horticultural produce is of high importance in the design of efficient handling and cooling systems. The objective of this research was to develop an airflow rate (AFR) measuring method that is more precise than a method previously developed and referred to as the Circular Approach Velocity (CAV) method, without modifying the airflow pattern. Instrumented balls used as produce simulators were calibrated to determine the correlations among their cooling rates (CR), cooling indexes (CI), air approach velocities, and AFRs. The applicability of the new method, referred to as the Square Cross Section Velocity (SCSV) method, using these instrumented balls as an indirect measurement method of air velocity was evaluated and compared to the CAV method. With the SCSV method, the relationships between the AFRs and the CRs were determined as a function of the position of the instrumented balls in reference to the air entrance. The two methods were evaluated by a comparison of the data obtained for three percentages of open area in packages (0.67, 2, and 6%) and six AFRs (ranging from 0.125 to 3.9 L s^{-1} kg^{-1} of produce), and the calculation of a mass balance. The comparison showed that the SCSV method was only slightly better at predicting variations in cooling rate than the CAV method, but was much better at predicting AFR than the CAV method. A statistical analysis was performed and demonstrated that only one replication of each of the six AFRs would have been sufficient to distinguish the effect of the AFR used on the cooling rate. However, three replications are required to discriminate between the significant effect of AFRs and the percentages of open area on the CR of individual produce products and the uniformity of the CR of a range of produce products across the porous medium. **Keywords**: produce simulator, container, forced-air cooling, half-cooling time, air approach velocity, precooling.

Savoir la forme de la distribution de l'air à l'intérieur d'un milieu poreux tels des produits horticoles en contenant est très important lors de la conception de systèmes de manutention et de refroidissement efficaces. L'objective de la présente recherche était de développer une méthode de mesure du débit d'air (AFR) plus précise que celle précédemment développée, appelée méthode de la vitesse d'approche circulaire (CAV), sans toutefois modifier le patron de distribution de l'air. Des balles instrumentées utilisées comme simulateur de produit ont été étalonnées pour déterminer la corrélation entre leur taux de refroidissement (CR)et leur indice de refroidissement (CI), et la vitesse d'approche de l'air et le débit total de l'air (AFR). L'applicabilité de cette nouvelle méthode, appelée méthode de la vitesse moyenne de la section carrée (SCSV) et utilisant ces sphères instrumentées, a été évaluée comme méthode indirect de mesure de la vitesse de l'air et comparée à la méthode CAV. Dans la méthode SCSV, la relation entre les AFRs et les CRs a été déterminée en fonction de la position des balles par rapport à l'entrée de l'air. Ces deux méthodes ont été comparées en calculant des bilans de masse sur les résultats obtenus en utilisant trois pourcentages d'ouverture pour l'entrée de l'air (0.67, 2 et 6%) et six débits d'air distribués entre 0.125 et 3.9 L s^{-1} kg^{-1} de produit. Cette comparaison a démontré que la méthode SCSV est légèrement meilleure pour prédire les différences de taux de refroidissement que la méthode CAV; par contre elle est de beaucoup performante pour prédire les AFR. Une analyse statistique a démontré qu'une seule répétition pour chacun des six débits d'air serait suffisante pour démontrer l'effet du AFR utilisé sur le taux de refroidissement. Toutefois, trois répétitions sont requises pour discriminer les effets du débit d'air et des ouvertures sur le taux de refroidissement d'un produit et l'uniformité des taux de refroidissement à travers une masse de produits formant un tel milieu poreux.

INTRODUCTION

Because of the significant amount of postharvest horticultural produce losses and increases in energy costs, intense research programs on maintaining good quality and on process efficiency have been matters of high interest for the past decade (Émond et al 1996; Goyette et al 1996; Alvarez and Flick 1999a, 1999b). Among postharvest processes, an optimal precooling process generally plays the most important role in achieving the goals of maintaining good quality and of process efficiency. The efficiency of the precooling process on maintaining produce quality depends on the rapidity and uniformity of temperature reduction. Heterogeneous cooling may cause moisture loss, freezing, or severe loss of quality due to microbial spoilage (Alvarez and Flick 1999b; Van der Sman et al. 1996). The efficiency of precooling systems affects the benefits experienced by producers because of the advantages of the extended shelf-life of produce and because acquisition and operation of the refrigeration system are as cost-effective as they can be. Cooling process efficiency, air pressure drop through the produce, and openings of the package affect the amount of energy required to operate the precooling system. Decreases in process efficiency and increases in air pressure are attributable to the type of produce, the percentage of open area, and the location of package openings, all of which affect the energy required to operate the precooling system (de Castro et al. 2005). The design of a container is critical to promote sufficient and uniformly distributed fluid around the produce during

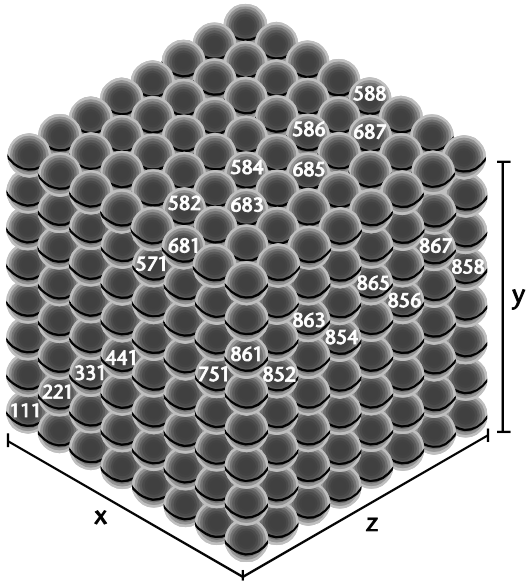

Fig. 1. Schematic representation of the cubic matrix of balls. The balls with numbers were instrumented and the number represents the position xyz of the ball in the matrix.

forced-air precooling (de Castro et al. 2004a, 2004b). The container must have enough open area to allow uniform and fast air circulation around the produce without affecting its mechanical resistance (Vigneault and Goyette 2002a, 2002b). A well-designed container must ensure adequate preservation of produce quality and prevent excessive energy input (Vigneault et al. 2002).

A wide variety of containers has been developed over time for the fresh fruit and vegetable market. However, the size of their openings and the locations of the openings seem arbitrary. Detailed recommendations for a standard container dedicated to fruit and vegetable handling have not yet been documented. The various existing recommendations are based on very specific experimental conditions and are sometimes contradictory (Van der Sman 2002; Vigneault et al. 2002; Kader 2002). Sufficient evidence about the influence of the positions of container openings on air distribution exists; nonetheless, contradictory conclusions as to whether they may produce significant effects on cooling efficacy appear in the literature (Leyte and Forney 1999; Émond et al. 1996; Smale et al. 2003).

An original concept was developed for the indirect measurement of air distribution as a function of container design, particularly the location of the openings, specifically for horticultural crop handling (Vigneault and de Castro 2005). The authors developed a regression relation between the mean air velocity around a produce simulator and the produce simulator cooling rates (CR) during the forced-air precooling process. The resulting method has the potential to become an accurate and useful tool to assist in the design of containers since it should allow for the precise measurement of air velocity profiles within containers of horticultural produce.

The objectives of the present research were: (1) to verify the applicability of this indirect airflow measuring method to revealing the airflow pattern around packed produce; (2) to develop a new avenue to increase the accuracy of indirect airflow measurement; (3) to determine a procedure to validate the results obtained; and (4) to determine the effect of the number of replications on the capacity of the experimental design to identify significant differences among treatments.

MATERIALS and METHODS

The research tool proposed by Vigneault and de Castro (2005) was developed to investigate the air distribution in containers during forced-air precooling. For the indirect measurement of the air approach velocity, these authors used a correlation between the mean air velocity surrounding a ball and two thermal characteristics of the balls, the CR and the cooling index CI. The CR (s^{-1}) is defined as the ratio of the change in the logarithm of the dimensionless time-temperature ratio of an object and the surrounding air. For this project, the CR was calculated using a dedicated ExcelTM macro described by Goyette et al. (1996).

The CI (s^{-1}) was defined by Vigneault and de Castro (2005) as the CR of the balls measured under predefined standard conditions. It is used to characterize each ball and to select only balls with similar thermal properties, thus reducing experimental error. Although thermal conductivity and diffusivity are more extensively used as material thermal properties, CI presents the advantage of taking into account variations among the physical characteristics of the balls such as radius, density, and specific heat (Vigneault and de Castro 2005).

The applicability of the indirect air velocity measuring method developed by Vigneault and de Castro (2005) was evaluated using the produce simulator described below.

Produce simulator

The horticultural produce simulator described in detail by Vigneault and de Castro (2005) consists of solid polymer balls measuring 52.36 mm in diameter and having a mass of 125.55 g. Sixty-four balls were selected for their relatively high uniformity in CI (-0.1414 ± 0.0081 min^{-1}) and heat capacity (1.1252 ± 0.0657 kJ kg^{-1} $°C^{-1}$). Each of the 64 balls was instrumented with a 30-gage 5 m-long insulated copper constantan thermocouple wire (Type T) placed in its centre with a precision of ±0.025 mm.

Experimental set-up

The 64 instrumented balls were stacked uniformly along with 448 other balls on a face-centered cubic packing pattern to form a matrix of eight balls per side (Fig. 1). Table 1 presents the orthogonal positioning reference system of the instrumented balls; the z axis corresponds to the airflow direction. The arrangement resulted in 47.64% porosity. The balls forming the two end layers in the "z" direction were joined together using plastic pins that were12 mm in length and 6 mm in diameter. The pins were inserted into 6-mm depth holes pierced at each ball to ball or ball to wall contact point. Thirty groups of five balls each were also assembled to form five-ball stars to ensure sufficient stability throughout the matrix. These five-ball stars were assembled using one centre ball surrounded by the four other balls in contact within a single geometric plane, using the same 12-mm long plastic pin assembling system, and distributed within the matrix.

Table 1. Locations of instrumented balls throughout the matrix.

Ball Code	X	Y	Z	Ball Code	X	Y	Z	Ball Code	X	Y	Z	Ball Code	X	Y	Z
1	1	1	1	17	1	1	3	33	1	1	5	49	1	1	7
2	2	2	1	18	2	2	3	34	2	2	5	50	2	2	7
3	3	3	1	19	3	3	3	35	3	3	5	51	3	3	7
4	4	4	1	20	4	4	3	36	4	4	5	52	4	4	7
5	7	5	1	21	7	5	3	37	7	5	5	53	7	5	7
6	8	6	1	22	8	6	3	38	8	6	5	54	8	6	7
7	5	7	1	23	5	7	3	39	5	7	5	55	5	7	7
8	6	8	1	24	6	8	3	40	6	8	5	56	6	8	7
9	2	1	2	25	2	1	4	41	2	1	6	57	2	1	8
10	1	2	2	26	1	2	4	42	1	2	6	58	1	2	8
11	4	3	2	27	4	3	4	43	4	3	6	59	4	3	8
12	3	4	2	28	3	4	4	44	3	4	6	60	3	4	8
13	8	5	2	29	8	5	4	45	8	5	6	61	8	5	8
14	7	6	2	30	7	6	4	46	7	6	6	62	7	6	8
15	6	7	2	31	6	7	4	47	6	7	6	63	6	7	8
16	5	8	2	32	5	8	4	48	5	8	6	64	5	8	8

Figure 2 shows the experimental set-up used during the trials. Four transparent acrylic plates were assembled to simulate a 1250 mm long forced-air cooling tunnel with a 420-mm inside square cross-section. The ball matrix was positioned at a distance of 220 mm from the tunnel's air-inlet end. The portion of the tunnel containing the balls was insulated with a 25 mm-thick polystyrene foam to reduce heat conduction. The air outlet of the tunnel consisted of a 610 mm-long plenum allowing measurements of air pressure drop (APD) across the ball matrix with a pressure transmitter in the range of 0-127±6 mm of water (Model 607-7, Dwyer Instruments Inc. Michigan City, IN).

The aspiration chamber was built from plywood that was 10-mm thick, and had outer dimensions of 900x600x600 mm. The tunnel's air-outlet end was attached to the aspiration chamber so as to be airtight. The aspiration chamber was divided into two inner compartments: an upper division and a lower division. A direct drive radial blade fan (Model PW-11, Peerless Electric, Hot Springs, NC,) driven by a 0.75 kW variable speed motor (Model G344, Marathon Electric, Wausau, WI) was fixed between the two inner divisions. A variable AC motor drive (Model M1215SB, AC Tech, Uxbridge, MA) connected to the motor allowed the proportional control of fan

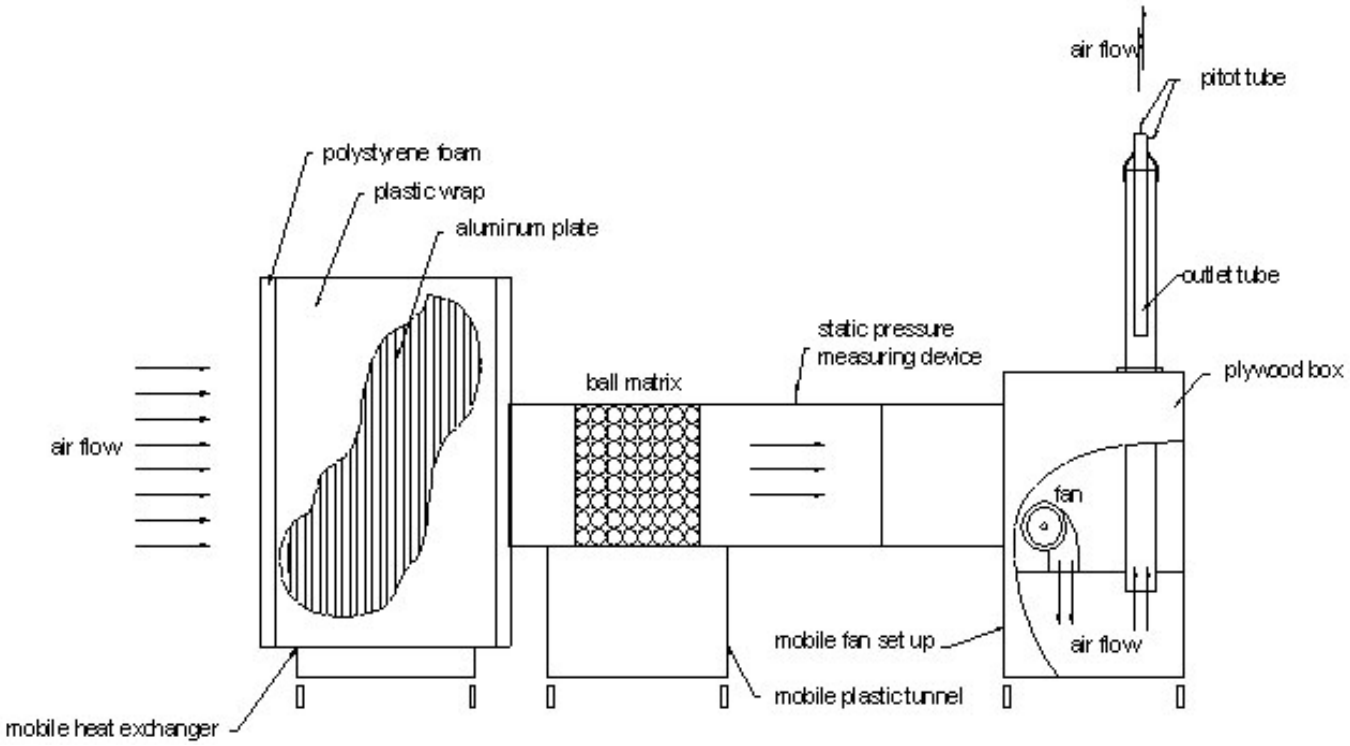

Fig. 2. Experimental set-up showing forced air tunnel, balls matrix, fan, and pressure measuring devices.

speed. The fan created a negative pressure in the upper division and forced the outside air to circulate through the cooling tunnel. The air was released to the atmosphere through a tube 500 mm in length and 101.6 mm in diameter, instrumented with a Pitot tube device allowing airflow measurements. Two transmitters, 0-12.7+0.6 mm of water and 0-25.4+0.13 mm of water (Models 607-2 and 607-3, Dwyer Instruments Inc. Michigan City, IN) were used to measure the static and total pressures at the Pitot tube. Two other tubes, 500 mm in length and 76.2 mm or 31.8 mm in inner diameter, were assembled in an airtight manner in the 101.6-mm diameter tube to measure lower airflow. These three tubes were used to provide acceptable measurements of the dynamic pressure. The whole experimental set-up was placed in a cold chamber maintained at 4 °C to simulate a precooling process by forcing ambient air to circulate through the ball matrix.

A fully open configuration was initially tested to determine the correlation between the half-cooling time (HCT) of the 64 produce simulators and air approach velocity. The HCT is defined as the time required to extract half of the energy contained in a produce product based on its initial temperature and the ambient temperature to which the product is exposed. The method used in the present work to calculate the HCT, based on a central temperature decreasing with time, was described in detail by Goyette et al (1996) and largely used by various authors (Goyette et al. 2000; Rennie et al. 2000; DeEll et al. 2000).

Based on the volume and the thermal mass of the ball matrix, six AFRs were chosen to cover the total range of air velocities encountered in the fruit and vegetable precooling process. These air velocities are equivalent to 0.125, 0.25, 0.5, 1, 2, and 3.9 L s^{-1} kg^{-1} of produce mass based on the mean produce density as described by Vigneault et al. (2004). Three other opening configurations were studied. A pair of plates was placed next to the first and eighth layers of balls to enclose the matrix within a simulated package of two perforated sides. The pair of square plates was made from 3-mm-thick, 420-mm-long polypropylene plates that were perforated with circular metal saws. Nine holes, each 38.7 mm in diameter or 0.67% of the total plate area, were uniformly distributed across the plate surface (Fig. 3). Three total opening areas (TOA) were evaluated and corresponded to 0.67, 2, and 6% of the plate area using the central hole, the central line of holes, or the nine holes, respectively. These configurations were obtained by creating airtight seals with tape over the other holes, as necessary.

The pressure drop obtained with the 1, 2, and 3.9 L s^{-1} kg^{-1} AFRs with the central hole configuration exceeded the capacity of the fan. Therefore, four AFRs were readjusted for this configuration to 0.125, 0.25, 0.5, and 0.75 L s^{-1} kg^{-1} . For similar reasons, the experiments with the plates with three holes were conducted only up to a 2 L s^{-1} kg^{-1} AFR. Furthermore, the transmitter upper-limit of 125 mm of water was set as the limit for pressure drop in the experiments, since higher values would not be considered as practical for commercial storage rooms (Kader 2002).

A 520x840x1100 mm thermal mass was built to minimize, during the experiments, temperature variation at the air inlet resulting from the variation of the cold chamber temperature. This thermal mass consisted of 30 perforated aluminum plates, each measuring 520x1100 mm and 1 mm in thickness, spaced 25 mm apart. These plates were uniformly perforated with holes 4.76 mm in diameter, resulting in a 44% open area. The plates were attached together and insulated longitudinally with a 50 mm-thick polystyrene foam. The lateral portions of the thermal mass were wrapped with plastic to prevent air infiltration. One end of this thermal mass was also insulated with a polystyrene frame to which the forced-air tunnel could be attached during experiments (Fig. 2). The air suctioned from the cold chamber by the fan was thus forced to circulate first through the thermal mass before reaching the balls.

Instrumentation and control

All instruments and motors in the experimental set-up were monitored and controlled using a data acquisition system (34970 Data Acquisition/Switch Unit – Agilent Technology, HP, Palo Alto, CA) via custom-made desktop software using VEE language (Agilent Technology, HP, Palo Alto, CA). Preliminary tests were performed to tune the control system; the relationship between the voltages required by the motor to provide a certain air velocity, with respect to the various numbers of openings, was determined and integrated into the software. The AFRs were calculated by computing the air velocity using the pressure velocity relationship (ASHRAE 2001) of the Pitot tube and proportionally adjusting the fan motor through the AC motor drive. At the start of each experiment, the user was prompted to input the opening distribution and the set point air velocity. The experiment was subsequently entirely automated. The temperature inside the 64 balls, the air temperature before and after the ball matrix was crossed, the temperature in the centre of the cold chamber, the pressure drop through the ball matrix and the plates, and the dynamic pressure of the air were simultaneously recorded at 20-s intervals. The set point velocity was maintained using a continuous error monitoring system that readjusted the fan voltage as necessary.

Experimental procedure

Each opening configuration was tested with the various AFRs and repeated three times. Prior to the start of each test, the forced-air tunnel containing the balls was placed in a warm chamber maintained at 27±1.0 °C. An axial fan circulated ambient air through the ball matrix for about 120 minutes, which resulted in a uniform temperature at the centres of the 64 instrumented balls. After this conditioning period, the perforated plates were installed and the tunnel was placed in the cold room. The tunnel's air-inlet end was connected to the aluminum thermal mass and the air outlet to the aspiration chamber. The centrifugal fan was turned on immediately. The data were recorded until the temperature of the warmest ball reached 6.9 °C, which corresponds to a complete precooling process (Goyette et al. 1996). At this point, the software terminated the control process and turned off all devices. The temperature-time data recorded were used to calculate the HCT and CR of each ball for all treatments using a dedicated ExcelTM macro developed by Goyette et al. (1996).

Air-mass balance research tool evaluation

Two methods for measuring the mean air approach velocity around an instrumented ball were compared. The first method, called the CAV method (Vigneault and de Castro 2005), consisted of using the general exponential correlation (Eq. 1)

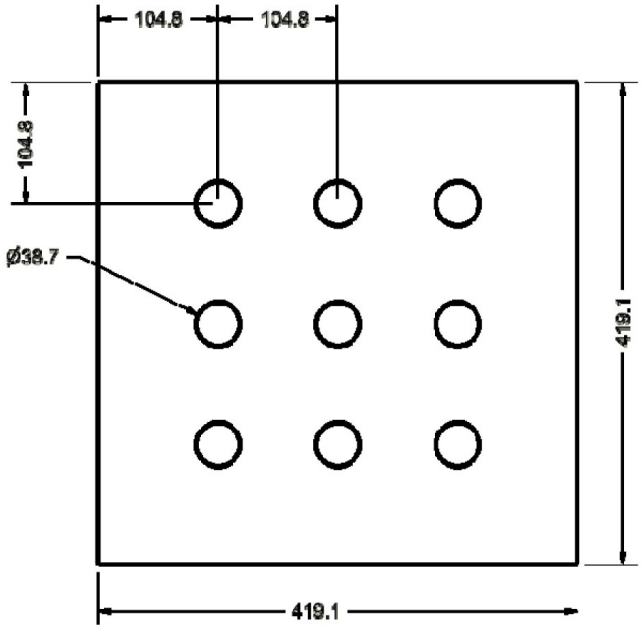

Fig. 3. Plastic plate with nine holes (38.7 mm diameter with each 0.67% open area) uniformly distributed.

between the cooling rate (CR, s^{-1}) of an instrumented ball and the mean air approach velocity (CAV, m/s) in the circular tube holding the ball. The diameter of the circular tube (D_t) used to obtain this correlation was $2\,D_b\pi^{-0.5}$, resulting in a cross-section of the circular tube that was equal to what a cross-section of a square tube of the same dimension as the diameter of the ball (D_b) would be.

$$CR = -0.02615\ln(CAV) + 0.6989CI \qquad R^2 = 0.9865 \qquad (1)$$

where:

CR = cooling rate of instrumented ball (min^{-1}),
CAV = mean air approach velocity (m/s), and
CI = cooling index.

Equation 1 was applied to calculate the air approach velocity from the CR of the 64 balls in the matrix. At the two lowest airflows (0.125 and 0.250 L s^{-1} kg^{-1}), the natural convection was predominant and produced CRs less than 0.025 min^{-1}. These values prevented the use of the correlation to establish air velocity profiles in this range of airflow (Vigneault and de Castro 2005).

In the second method, called the SCSV method, the fully open matrix was submitted to the six AFRs previously mentioned and the HCT (min) was determined for each ball. A mean air approach velocity in a square cross section (SCSV, m/s) was calculated by dividing AFRs by the cross-section of the forced-air cooling tunnel. A specific correlation was developed to explain the relation between the AFR and the CR of each ball. The new equations thus included the specific thermal properties of each ball (Vigneault and de Castro 2005) and the variability of the air movement around each ball according to its specific position in the matrix.

Both methods were used to infer the AFR at the 64 positions inside the container from the HCT. The two methods were evaluated with the data obtained for the three container opening areas (0.67, 2, and 6%), and the AFRs ranging from 0.125 to 3.9 L s^{-1} kg^{-1}. The mass of air circulation around each ball was calculated based on the assumption of a vertical and horizontal symmetry of air circulation. Therefore, the velocities of the air around the other positions occupied by the 56 non-instrumented balls in each layer on the z-direction were determined from the hypothesis of symmetry in x and y directions. The calculation based on each of the two methods thus resulted in empirical measurements of the masses of air crossing each z-direction layer. The total masses of air measured with these two indirect airflow measuring methods were compared to the mass of air measured by the airflow measuring device through a Tukey test using SPSS v. 11.5 (SPSS Inc. 2004. Chicago, IL)

The air-mass balance analysis considered the AFR obtained with the fully open configuration data from the areas surrounding the balls contained in each z-direction layer. Therefore, a one-way ANOVA and Tukey test were performed on SPSS v. 11.5 to identify any significant differences among the masses of air calculated in each z-direction layer using the two indirect measuring methods.

Outlier rejection

A result validation procedure was developed based on the identification and rejection, within a confidence level of 99.9%, of any HCT replication standard deviation larger than the outlier upper limit, which is equal to the mean standard deviation plus 3.09 standard deviations (Montgomery 1996). Thus, the standard deviation of the HCT was calculated for each ball and plotted as a function of the AFR. A regression equation was calculated and the outlier upper limit was calculated for each AFR. The outliers were identified and rejected. New regression equations and outlier upper limits were determined from the remaining HCT results and so on, until any outlier was identified as recommended by Montgomery (1996).

Number of replications

The determination of the effect of the number of replications on the capacity of the experimental design to identify significant differences among treatments was performed based on Eq. 2.

$$d^2 = \frac{Fs}{n} \qquad (2)$$

where:

F = tabulated Fisher-Distribution value for desired confidence level and the degree of freedom of the initial sample,
n = number of replications,
s^2 = variance of the samples, and
d = half-width of the resulting confidence interval (Steel and Torrie 1980).

RESULTS

In general, the whole set up, including all the measurements, control systems, and software allowed practical procedures and precise performance quantification when the experiments were executed. The results obtained for HCT, CR, and AFR calculated from the temperature variation at the centre of each of the 64 instrumented balls inside the matrix for each opening

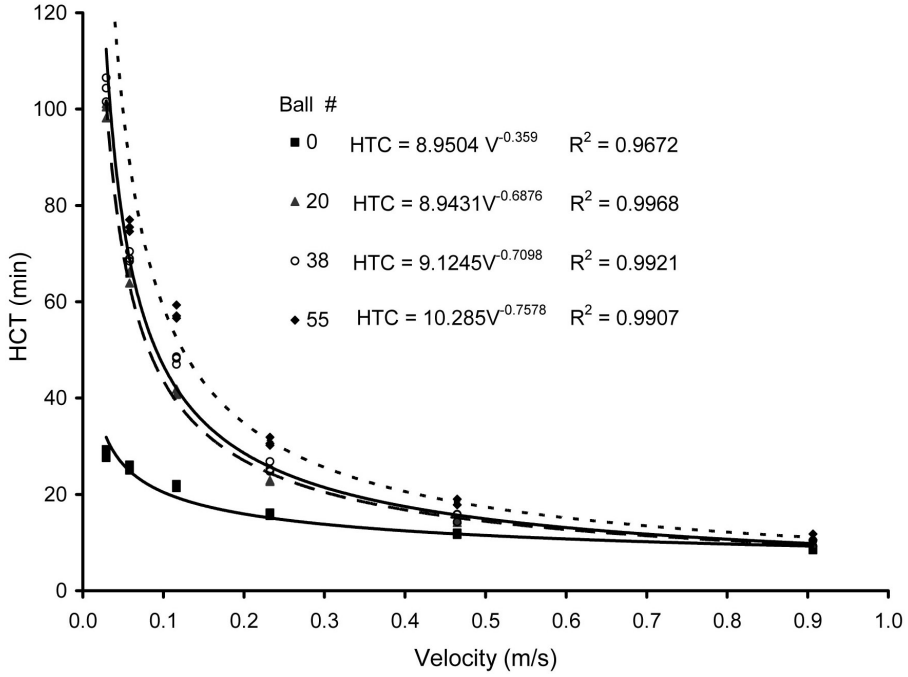

Fig. 4. HCT responses for balls 1, 21, 39, and 56 from layers z = 1, 3, 5, and 7, respectively.

configuration and AFR were replicable. The consistency of the results obtained using the instrumented balls is an advantage of the indirect airflow measurement method compared to the direct measurement method used by Alvarez and Flick (1999a, 1999b) which was highly position dependent.

The HCTs obtained for four randomly chosen balls (1, 21, 39, and 56) from the odd z-layers of the fully-open configuration (1, 3, 5, and 7, respectively) are presented in Fig. 4, as examples. The experimental system produced good relationships between the HCTs and the AFRs of all ball positions since the smallest regression goodness of fit coefficient (R^2) was 0.9589 (result not presented). The fully-open configuration also showed the significant effect of AFRs on the variance of HCTs ($F_{5,\ 378}$ = 9.692, P<0.0005). The highest variances obtained corresponded to the minimum AFR (0.125 L s^{-1} kg^{-1}).

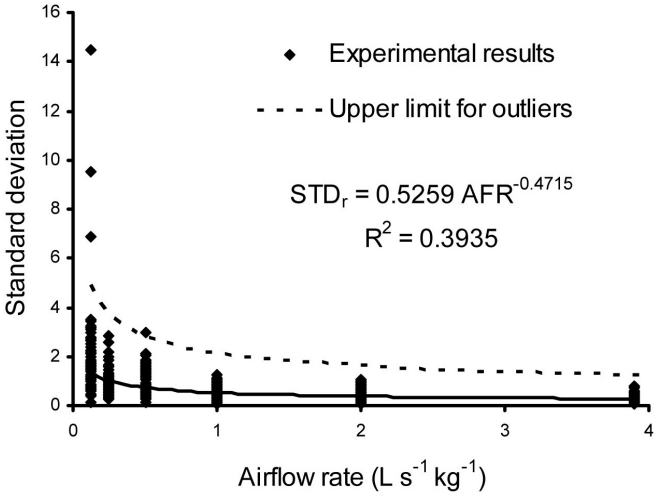

Fig 5. Effect of AFR on the mean standard deviation (STD_r) of the HCT responses, including the four outliers.

Effect of airflow rate on replication standard deviation

Equation 3 shows the effect of the AFRs on the replication standard deviation. The AFR explains 93.41% of the replication standard deviations.

$$STD_r = 0.6326 AFR^{-0.4538}$$

$$R^2 = 0.9341 \qquad (3)$$

where: STD_r = replication standard deviation

Equation 3 was used to calculate the mean standard deviation of the results corresponding to each AFR and to determine the outlier limits.

Outlier rejection

Among the 1152 HCTs calculated (3 replicates, 6 AFRs, 64 balls), only four results were rejected as outliers, identifiable by the Montgomery (1996) method (Fig. 5). Three outliers were from the lowest AFR tested, likely showing that using very low AFRs would yield variability and instability in the experimental results. In fact, the variability increased when the AFRs decreased (Table 2). The fourth outlier was from the 0.5 L s^{-1} kg^{-1}, which shall be discussed presently. The remaining data obtained from the fully-opened configuration were used to establish the specific correlation between the AFR and the HCT of each ball positioned at a permanent location in the matrix (Fig. 6).

The outlier rejection validation technique was also performed to identify and reject any other outliers from the other opening configurations. When it was possible, the causes producing outliers or incorrect results during the subsequent experiments were identified and the experiments were corrected.

Table 2. Minimum difference between two HCT results for them to be considred as significantly different at a confidence level of 95% (alpha = 0.05) for the various AFRs.

Airflow rate (L s^{-1} kg^{-1})	S^2	Md_1* (min)	Md_2 (min)	Md_3 (min)	Md_4 (min)
0.125	3.527	3.72	2.33	1.78	1.48
0.25	1.859	2.71	1.70	1.30	1.08
0.50	0.979	1.98	1.24	0.95	0.79
1.00	0.516	1.45	0.91	0.69	0.58
2.00	0.272	1.06	0.66	0.51	0.42
3.90	0.147	0.78	0.49	0.37	0.31

*Md_x = minimum difference when using x replicates (x = 1, 2, 3, or 4)

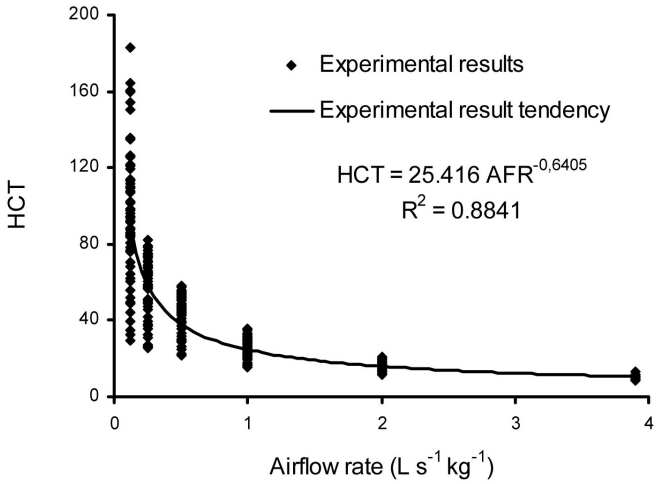

Fig. 6. Mean-replication effect of AFR on the HCT responses after the four outliers were rejected.

Number of replications

The effects of the number of replications (n) on the capacity of the experimental design to identify significant differences between treatments is presented in Table 2. As expected, the minimum difference that needed to be observed between two HCTs for results to be considered as significantly different at a confidence level of 95% decreased with the increase of AFRs and the number of replications. These results could be used to determine the number of replications required to demonstrate the effects of any AFR or opening configuration, as long as the expected mean and variance of two experimental conditions were known. In the present study, one replication of each of the six AFRs would have been sufficient to discriminate the effect of the AFR used. However, three replications were necessary to discriminate among the effects of various opening configurations.

Evaluation of the research tool based on air-mass balance

CAV method Equation 1 explained 98.65% (R^2) of the variation in the CRs of the balls (CR, min^{-1}) as a function of the circular-area mean air approach velocity (CAV, m/s) and the CI of each ball (min^{-1}) (Vigneault and de Castro 2005). Equation 4, used to calculate the mass balance according to the CAV, was developed from Eq. 1 and the relation between half cooling time (HCT, min) and CR (min^{-1}) (Eq. 5) (Goyette et al. 1996).

$$CAV = \exp(26.73CI + 26.51 / HCT) \quad (4)$$

$$HCT = \ln(0.5) / CR \quad (5)$$

The mean air velocities based on the CAV produced a mass balance explaining 92.9% of the variation of the AFRs measured mechanically and showed a significant correlation between the results of these two measuring methods ($F_{6, 353}$ = 610.2, P<0.0005). However, there were no significant differences between the air velocities calculated with that CAV method in the AFR range of 0.125 to 0.5 L s^{-1} kg^{-1}, nor were any significant differences detected between the air velocities calculated at 0.5 and 0.75 L s^{-1} kg^{-1}, and at 0.75 and 1 L s^{-1} kg^{-1} (Table 3). Finally, the CAV method always produced lower AFR results than the AFRs measured mechanically. This lower result could be explained by the methodology used during the calibration of the CAV method, which considered only one ball being cooled at a time. The air circulating around the ball therefore did not meet any obstacles and moved fairly well all around the surface of the ball. However, when the test was performed using the AFR through the ball matrix, the actual surface of the ball directly exposed to cold air was considerably reduced. In fact, in a face-centered cubic packing pattern, the balls touch six other objects (other balls, plastic slabs or tunnel walls), creating several obstructions to air circulation. These obstructions generate a higher HCT than the value that would have been reached in the absence of any obstruction. The higher HCT in turn results in lower AFR calculations.

Table 3. Tukey test showing the effect of the measured AFRs on the air velocity results obtained from each method applied on the results of 0.67, 2, and 6% open areas.

Measured velocity (m/s)	Airflow rate (L s^{-1} kg^{-1})	Number of samples	SCSV velocity (m/s)	CAV velocity (m/s)
0.029	0.125	72	0.022 a*	0.029 a
0.058	0.25	72	0.055 b	0.036 a
0.116	0.50	72	0.114 c	0.048 ab
0.174	0.75	24	0.171 d	0.060 bc
0.232	1.00	48	0.244 e	0.076 c
0.465	2.00	48	0.507 f	0.151 d
0.906	3.90	24	1.019 g	0.418 e

* Means followed by the same letter in the same column are not significantly different at α = 0.05

SCSV method The mass balance based on SCSV (m/min) was based on the 64 equations developed from the whole matrix in the fully open configuration submitted to the six AFRs. A regression analysis was performed (Eq. 6a) and showed a good overall correlation (R^2=0.8841) when the results as a whole were considered (Fig. 6). Individual ball performances were then used to determine a correlation equation between air velocity (SCSV, m/min) and the half-cooling time (HCT, min) for each ball (Eq. 6b). The 64 resulting equations explained 98.77 ± 0.89% (R^2) of the variations of the CRs of the balls for the operating conditions tested. The a and b empirical parameters and individual goodness of fit coefficients (R^2) of eight equations are presented in Table 4, as examples. These equations were then used to produce the air mass balance according to the SCSV method.

$$HCT = 25.416 SCSV^{-0.6406} \quad R^2 = 0.8841 \quad (6a)$$

$$HCT = a\, SCSV^{b} \quad R^2 = 0.9877 \pm 0.0089 \quad (6b)$$

The results of this mass balance demonstrated that when the cross-section area of the ball matrix is taken into account, the mean air velocity around each instrumented ball can be determined. The mean air velocities based on the SCSV produced a mass balance explaining 99.3% of the variation of the AFRs measured mechanically and showed a significant

Table 4. Examples of goodness of fit coefficient and empirical parameters relating the HCT to the air approach velocity calculated according to the SCSV method for eight of the balls used to form the matrix.

Ball code	a	b	R^2
1	8.950	0.3590	0.9672
8	9.161	0.5027	0.9808
16	10.121	0.5413	0.9774
24	10.083	0.6154	0.9866
32	11.903	0.5951	0.9792
40	11.287	0.6418	0.9786
48	13.374	0.5976	0.9734
56	11.439	0.6403	0.9736

correlation between the results of these two measuring methods ($F_{6, 353}$ = 4405.2, P<0.0005). The SCSV method allowed the distinction of the significant differences among the air velocities that were calculated and that corresponded to the AFRs tested (Table 3).

Finally, the higher level of correlation achieved with SCSV equations, compared to the CAV results, suggests that this method should be used as the indirect airflow measuring method since it estimates the air mass flowing through the ball matrix more accurately than the CAV method.

Air-mass balance in z-direction

Lower CAV values were calculated at the z=8 layers and showed a significant negative Pearson correlation with z-direction at 0.05 level ($Pearson_{144}$ = -0.175, $P_{2\text{-tailed}}$ =0.036). These results were likely due to the use of solid balls producing a thermal mass effect.

The SCSV approach developed included the warming effect of the air as it crossed the matrix and reached the balls at the rear layers. Therefore, the SCSV approach validated the velocity symmetry hypothesis assumed for the z-depth direction

Table 5. One-way ANOVA level of significance for the difference between the mass balance calculated using the SCSV and CAV methods for each z-direction layer and AFR.

Method	Airflow rate (L s^{-1} kg^{-1})	Degrees of freedom	F	P
SCSV	0.125	7, 16	35.080	<0.001
	0.25	7, 16	27.341	<0.001
	0.5	7, 16	12.495	<0.001
	1	7, 16	3.689	0.015
	2	7, 16	1.069	0.426
	3.9	7, 16	1.767	0.164
CAV	0.125	7, 16	9409.762	<0.001
	0.25	7, 16	1574.059	<0.001
	0.5	7, 16	1512.670	<0.001
	1	7, 16	548.864	<0.001
	2	7, 16	127.795	<0.001
	3.9	7, 16	17.156	<0.001

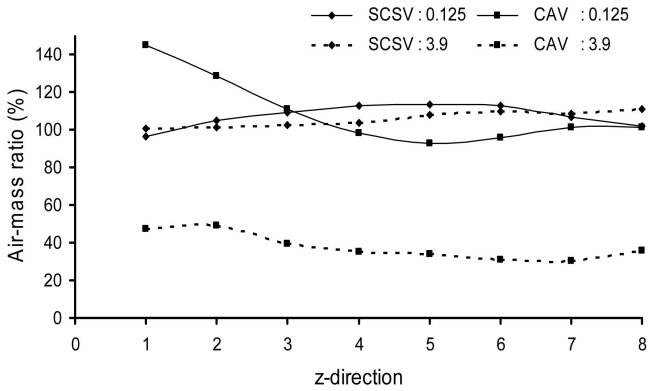

Fig. 7. Percentage of the total mass of air measured by the two indirect air velocity measuring methods (CAV and SCSC) for each z-direction layer for the minimum and maximum airflow tested (0.125 and 3.9 L s^{-1} kg^{-1}).

and did not show any air-mass significant correlation with z-direction ($Pearson_{144}$ = 0.010, $P_{2\text{-tailed}}$ =0.908).

An analysis of variance for both SCSV and CAV was performed for each z-direction at each AFR (Table 5). For SCSV, the position of the ball in the z-direction had a significant effect on the measurement of the AFR when it ranged from 0.125 to 1 L s^{-1} kg^{-1}. This global difference was generally due to the significant difference between the first layer (z=1) and the other z layers. For 1 L s^{-1} kg^{-1}, the velocities obtained in the z=1 layer were only significantly higher than the values found in the z=8 layer. The CAV air velocities showed significant differences among the eight layers for all AFRs tested (Table 5).

The graphic of the percentage of the total mass of air calculated at each z-layer for the minimum and maximum AFRs tested, by both indirect air velocity measuring methods, showed a dramatic increase in the accuracy of the indirect measurement of the AFR when the SCSV method was used (107.4 ± 5.94 and 105.8 ± 5.75%, respectively) compared to when the CAV method was used (109.3 ± 17.49 and 37.7 ± 7.16%) (Fig. 7). Furthermore, the results obtained from the SCSV method were fairly close to the results obtained from the Pitot tube measuring method for each z-direction layer. The SCSV method generated a 100.99 ± 9.18% overall average measurement of the air mass, but yielded significantly different results when AFRs were varied (Fig. 8). The same figure shows an increase of mass balance performance as the AFRs increased. In fact, lower results were obtained fairly often when testing at 0.5 L s^{-1} kg^{-1} , yielding a 85.77% mass balance difference. This lower result is explained by the underestimation of the regression equation of the HCT as a function of the AFR at this particular AFR (Fig. 9). The calculation of the Reynolds number for an AFR of 0.5 L s^{-1} kg^{-1} results in a value of 2081, which corresponds to the transition phase of an AFR from laminar to turbulent pattern. A specific study should therefore be performed to clarify the correlation between HCTs and AFRs in this particular case to increase the accuracy of the set-up.

The performance of the SCSV method is considered to be very good for an indirect measurement method of physical phenomena when compared to the mean precision of 77% obtained by Vigneault et al. (1992), which was already

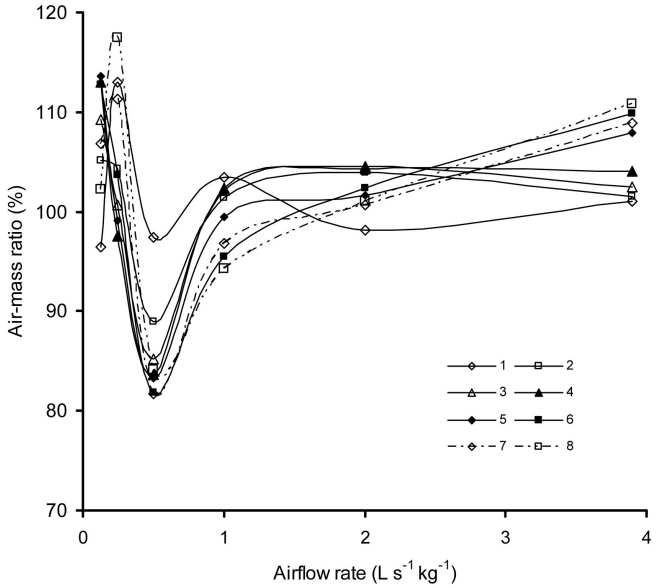

Fig. 8. Percentage of the total mass of air measured by the SCSV indirect air velocity measuring method for each z-direction layer as a function of the various AFRs.

considered as a fairly good result (Orsat et al. 1993). Furthermore, the SCSV indirect measurement method produced considerably more precise and stable results and had less disturbing effect on the airflow pattern than the aluminum sphere method or direct measurement method presented by Alvarez and Flick (1999a, 1999b).

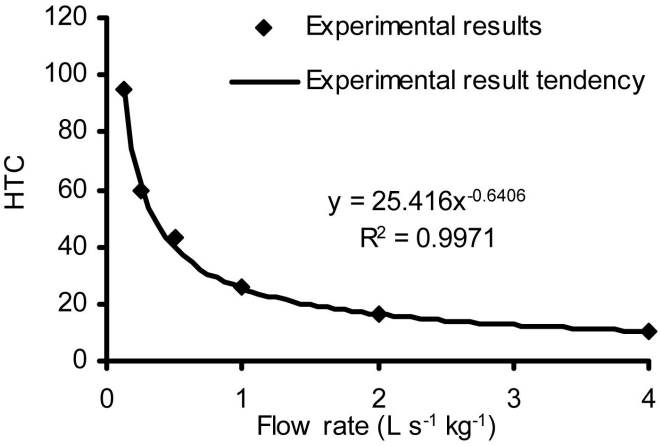

Fig. 9. Effect of airflow rate on the HCT responses based on the result averages.

Experimental set-up performance

The experimental method allowed the AFR effects to be distinguished. In fact, using only one replication would have been sufficient to accomplish this distinction. Some effects of opening configurations were also distinguished. The analysis of variance showed that the opening area had a significant effect on the variance of HCT ($F_{3,1340}$= 115.047, P<0.0005). Furthermore, the results obtained demonstrate the following:

- The variance increases as the opened area is reduced.
- No significant difference is found between the data for openings of 6 and 100%.
- At the minimum opening configuration (total surface area = 0.67%), the AFR has a significant effect on the HCT variance ($F_{3,252}$ = 22.47, P<0.0005). The highest variation is observed for the data produced with an AFR of 0.5 L s^{-1} kg^{-1}.
- The 0.125 and 0.25 L s^{-1} kg^{-1} AFRs produce the lowest variance of all the rates tested in this study.

The performance obtained showed the great potential of the experimental set-up and the SCSV method to distinguish the various effects of AFRs from opening configurations. Further research is necessary to define these effects; however, the experimental set-up is considered as capable of identifying the significant differences between the effects resulting from using various AFRs and configurations of opening.

CONCLUSION

Two indirect AFR measuring approaches were studied for their applicability in investigating airflow profiles through porous media. An experimental set-up allowed calibration of both methods. Application of statistical methods permitted the elimination of some experimental error and reduced the number of replications required to determine the significant effects of AFRs and opening configurations.

The use of the indirect measurement of the air velocity based on the CAV method showed some limitations. Moreover, this method did not produce accurate results, likely due to the thermal-mass effect.

The SCSV method improved the measurement of airflow pathways since it considered the variability of the air movement in various positions in the porous medium and resulted in a more accurate mass balance through the different layers in the direction of the airflow. This method allowed a consistent and precise determination of the air approach velocities for the package opening areas and AFRs investigated.

The effect of the number of replications on the capacity of the experimental design showed significant differences between the two treatments. In the current study, only one replication of each of the six AFRs would have been sufficient to distinguish the effect of the AFR used. However, three replications were necessary to distinguish the effect of various opening configurations.

ACKNOWLEDGEMENTS

This project was accomplished with financial support from the Horticultural Research and Development Centre of Agriculture and Agri-Food Canada and the Fundação de Amparo à Pesquisa do Estado de São Paulo (FAPESP). The authors thank Sandra Hindson and Tracy McLeod for their help during the preparation of the article and Mickey Waxman for technical support during the statistical analysis.

REFERENCES

Alvarez, G. and D. Flick. 1999a. Analysis of heterogeneous cooling of agricultural products inside bins. Part I: Aerodynamic study. *Journal of Food Engineering* 39: 227–237.

Alvarez, G. and D. Flick. 1999b. Analysis of heterogeneous cooling of agricultural products inside bins. Part II: Thermal study. *Journal of Food Engineering* 39: 239–245.

ASHRAE. 2001. *Fundamentals Handbook.* Atlanta, GA: American Society of Heating, Refrigerating and Air Conditioning Engineers, Inc.

de Castro, L.R., C. Vigneault and L.A.B. Cortez. 2004a. Container opening design for horticultural produce cooling efficiency. *International Journal of Food, Agriculture and Environment* 2(1): 135–140.

de Castro, L.R., C. Vigneault and L.A.B. Cortez. 2004b. Effect of container opening area on air distribution during precooling of horticultural produce. *Transactions of the ASAE* 47(6):2033–2038.

de Castro, L.R., C. Vigneault and L.A.B. Cortez. 2005. Effect of container openings and airflow on energy required for forced air cooling of horticultural produce. *Canadian Biosystems Engineering* 47: 3.1–3.9.

DeEll, J.R., C. Vigneault and S. Lemerre. 2000. Water temperature for hydrocooling field cucumbers in relation to chilling injury during storage. *Postharvest Biology and Technology* 18 (1): 27–32.

Émond, J.P., F. Mercier, S.O. Sadfa, M. Bourré and A. Gakwaya. 1996. Study of parameters affecting cooling rate and temperature distribution in forced-air precooling of strawberry. *Transactions of the ASAE* 39(6): 2185–2191.

Goyette, B., C. Vigneault, B. Panneton and G.S.V. Raghavan. 1996. Method to evaluate the average temperature at the surface of a horticultural crop. *Canadian Agricultural Engineering* 38(4): 291–295.

Goyette, B., C.K.P. Hui and C. Vigneault. 2000. An improved continuous liquid-ice system based on submerged mixing of water and ice. *Applied Engineering in Agriculture* 16(3): 259–263.

Kader A.A. (ed) 2002. *Postharvest Technology of Horticultural Crops*, 3rd edition. Publication No. 3311. Davis, Ca: University of California Division of Agricultural and Natural Resources

Leyte, J.C. and C.F. Forney. 1999. Optimizing flat design for forced-air cooling of blueberries packaged in plastic clamshells. *HortTechnology* 9(2): 202–205.

Montgomery, D. 1996. *Design and Analysis of Experiments*, 2nd edition. New York, NY: John Wiley & Sons.

Orsat, V., C. Vigneault and G.S.V. Raghavan. 1993. Air diffusers characterization using a digitized image analysis system. *Applied Engineering in Agriculture* 9 (1): 115–121.

Rennie, T.J., G.S.V. Raghavan and C. Vigneault. 2000. Determination of the product refrigeration load in vacuum cooling lettuce. *Applied Engineering in Agriculture* 16(5):459–464.

Smale, N.J., D.J. Tanner, N.D. Amos and A.C. Cleland. 2003. Airflow properties of packaged horticultural produce — A practical study. *Acta Horticuturae* 599: 443–450.

Steel R.G.D. and J.H. Torrie. 1980. *Principles and Procedures of Statistics: A Biometrical Approach*, 2nd edition. New York, NY: McGraw Hill Book Company.

Van der Sman, R.G.M. 2002. Prediction of airflow through a vented box by the Darcy-Forcheheimer equation. *Journal of Food Engineering* 55: 49–57.

Van der Sman, R.G.M., R.G. Evelo, E.C. Wilkinson and W.G. Van Doorn. 1996. Quality loss in packed rose flowers due to Botrytis cinerea infection as related to temperature regimes and packaging design. *Postharvest Biology and Technology* 7: 341–350.

Vigneault, C. and L.R. de Castro. 2005. Produce-simulator property evaluation for indirect airflow distribution measurement through horticultural crop package. *International Journal of Food, Agriculture and Environment* 3(2): 93–98.

Vigneault, C. and B. Goyette. 2002a. Design of plastic container openings to optimize forced-air precooling of fruits and vegetables. *Applied Engineering in Agriculture* 18(1): 73–76.

Vigneault, C. and B. Goyette. 2002b. Largeur des ouvertures au fond de contenants de plastique utilisés pour la manutention des produits horticoles frais. *Canadian Biosystems Engineering* 44: 3.7–3.10.

Vigneault, C., B. Panneton and G.S.V. Raghavan. 1992. Image analysis of 3-D clouds of bubbles. *Canadian Agricultural Engineering* 34 (4): 347–352.

Vigneault, C., M.R. Bordint and R.F. Abrahão. 2002. Embalagem para frutas e hortaliças. In *Resfriamento De Frutas E Hortaliças*, eds. L.A. Cortez et al., 95-140. Brasília, DF, Brésil: Embrapa Informaçã Tecnológica.

Vigneault, C., N.R. Markarian, A. da Silva and B. Goyette. 2004. Pressure drop during forced-air circulation of various horticultural produce. *Transactions of the ASAE* 47(3): 807–814.